Supplementary information for Conformal Metamaterial Inspired Contact Lenses - Designing, 3D Printing and Characterization for Ocular Applications

Haider Butt [a, b, 一二], Mohammed Ayaz Uddin [a,†], Muhammed Hisham [a], Valentyn S. Volkov [c]

[a] Department of Mechanical and Nuclear Engineering, Khalifa University of Science & Technology, Abu Dhabi, UAE.

[b] Advanced Digital & Additive Manufacturing (ADAM) Research Group, Khalifa University of Science & Technology, Abu Dhabi, UAE.

[c] Emerging Technologies Research Center, XPANCEO, Dubai Investment Park First, Dubai, UAE.

[一] Corresponding author. Email address: haider.butt@ku.ac.ae

[二] These authors contributed equally to this work

S1. Design Evolution and Rationale for the Auxetic-Inspired metamaterial Ocular lens

The motivation for this work originated from a persistent limitation in 3D-printed contact lenses, the appearance of slicing-induced edge artifacts, which arise inherently from layer-wise fabrication. These unintended circumferential ridges significantly compromise optical clarity and wearer comfort. To eliminate this problem, we adopted a "flat-to-fit" design philosophy, wherein the lens is fabricated as a flat disc and subsequently conforms to the hemispherical curvature of the cornea through structural, rather than material, mechanisms. This required a fundamental redesign of the lens architecture.

Geometric Foundations: Why a Flat Disc Cannot Become a Hemisphere

The design problem is rooted in classical differential geometry. A flat circular disc is a two-dimensional (2D) surface with zero Gaussian curvature, whereas the cornea approximates a three-dimensional (3D) hemispherical surface exhibiting positive Gaussian curvature at every point [1]. According to Gauss's Theorema Egregium, Gaussian curvature is an intrinsic property and cannot be altered through isometric deformation; that is, a flat surface cannot be smoothly transformed into a curved one without wrinkling or tearing. Fig. S1a demonstrates the challenge. This is the same geometric obstacle encountered in cartography when projecting a spherical Earth onto a flat map [2], [3]. Recognizing this intrinsic incompatibility clarified that a monolithic flat hydrogel disc would never wrap a hemisphere without distortion, regardless of material softness. Therefore, the geometry had to be fundamentally re-engineered (Scope of this study).

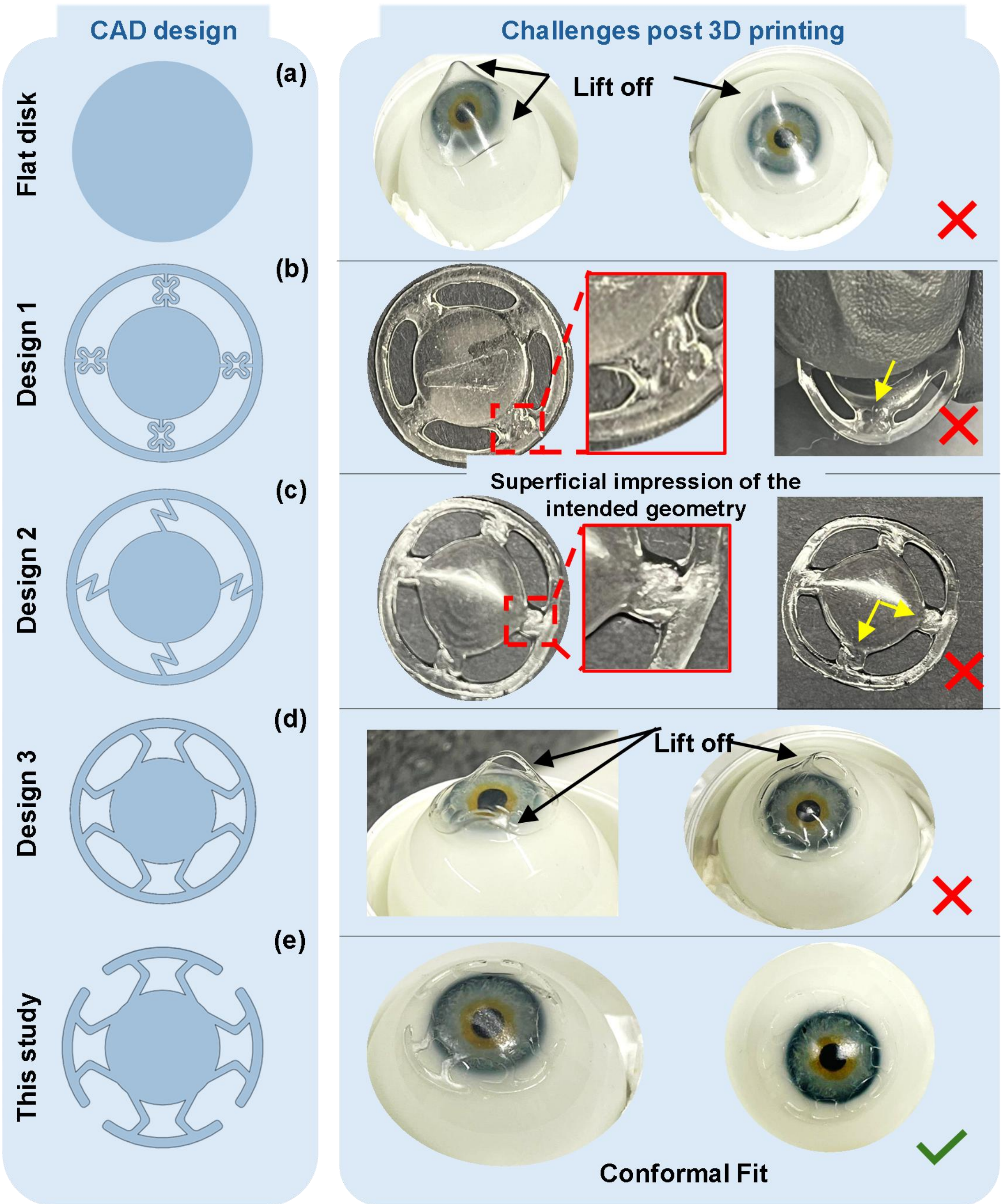

Figure S1: Design evolution of the ocular disc and its fit assessment on an eyeball model, demonstrating progressive improvements and revealing the key challenges associated with each iteration.

Conceptual Shift: From Monolithic Disc to Morphing Structure

To overcome curvature incompatibility, the design strategy shifted toward introducing a controlled geometric freedom within the disc enabling it to morph into 3D curvature while maintaining a planar printing configuration.

Two critical constraints guided this evolution:

i. The optical zone (8 mm diameter) must remain structurally intact to maintain refraction and visual performance.

ii. The surrounding architecture must provide controlled, compliant deformation allowing hemispherical wrapping.

This led to the first conceptual design: a flat disc with foldable radial ligaments and a circumferential supporting ring intended to enable self-folding and stretch-on-contact behavior (Fig. S1b-d).

Fabrication Constraints and Iterative Refinement

The initial prototypes of flat disc with foldable radial ligaments and a circumferential supporting ring revealed key practical constraints. Although the conceptual geometry supported stretchability, DLP printing limitations particularly related to minimum feature size hampered the fabrication of extremely thin foldable ligaments. Early attempts exhibited blury features, curing resin stuck in between the features, and loss of dimensional fidelity of the features. This behaviour indicates a resolution limitation and unintended light bleed during the printing process, resulting in overcuring and producing only a superficial impression of the intended geometry. (Fig. S1b-c).

While one design (Fig. S1d) printed successfully, the continuous circumferential ring imposed a structural coupling between ligaments. This meant that stretching or folding in one region introduced unwanted tension across the entire circumference, reintroducing the same conformability limitations inherent to the original flat disc as shown in Fig. S1d.

Final Breakthrough: Decoupled Quadrant Ligament Architecture

The decisive improvement came from removing the continuous circumferential constraint and decoupling the ligaments into four independent quadrants (see Fig. S1e). Introducing controlled spacing between quadrants allowed each ligament set to deform locally, without transmitting strain to the full perimeter.

This geometric decoupling produced three major benefits:

i. Localized adaptability: Each quadrant stretches or folds independently to conform to local curvature.

ii. Reduced global stiffness: Eliminating the circular ring minimized hoop stresses that previously resisted conformal wrapping.

iii. Metamaterial-like deformation modes: The architecture now behaved as a geometry-driven deforming lattice, consistent with mechanical metamaterial and auxetic design principles (see Fig. 2, Main Manuscript).

The final structure demonstrated reliable printability and excellent conformability, attributes essential for a flat-printed lens to transform into a 3D, curvature-matched ocular surface as shown in Fig. S1e.

Positioning as a Metamaterial-Inspired, Auxetic-Inspired Design

The evolution culminated in a design that does not rely on the bulk hydrogel properties alone. Instead, the compliance, curvature adaptability, and load-redistribution characteristics arise from its geometry, a hallmark of mechanical metamaterials. The rotational and stretching behavior of the ligament units mimics the deformation modes of classical auxetic architecture, even without achieving a true negative Poisson's ratio as explained in following discussion.

The proposed flat ocular disc is intentionally engineered using principles derived from mechanical metamaterials and auxetic architectures, where geometry but not material composition governs deformation. While we do not claim that the design exhibits auxetic nature, its functionality is inspired by the deformation mechanisms characteristic of auxetic systems, particularly those relying on rotational units, hinge-like elements, and arc-length-expanding motifs. These geometric features enable unconventional compliance, curvature adaptability, and shape transformation that cannot be achieved through polymer softness alone.

The disc incorporates a network of circumferential ligaments surrounding a fixed central optical zone. Each ligament contains a narrowed hinge region edged by terminal segments, forming a rotational, re-entrant like unit (see Fig. S1e). When the flat disc is applied to a hemispherical cornea or subjected to conformity testing, these ligaments undergo outward rotation and geometric unfolding as demonstrated in Video S1. This rotation increases the effective circumferential arc length, enabling the disc to accommodate the cornea's positive Gaussian curvature without wrinkling, tearing, or imposing stress concentrations at the central optical region. Such kinematic expansion through coordinated ligament rotation closely parallels the deformation pathways observed in auxetic-inspired architectures as demonstrated in Video S2 and Video S3. Upon placement on a hemispherical cornea, these units do not simply elongate; they undergo outward rotation, geometric unfolding, and effective circumferential arc-length expansion kinematic features widely associated with auxetic-inspired systems. This mechanism permits perimeter growth without tearing, wrinkling, or stress localization, demonstrating that the auxetic inspiration is rooted in the deformation as shown in Video S1 and Fig. 2, Main Manuscript.

Importantly, the disc's curvature-adaptive behavior arises primarily from architected geometric freedom apart from bulk hydrogel elasticity. This aligns with the defining characteristics of mechanical metamaterials; wherein mechanical function is embedded within the topology of the structure. By decoupling deformation into quadrant-wise rotational units, the design minimizes global hoop stiffness, enhances local adaptability, and ensures smooth planar-to-hemispherical transitions while preserving optical center region (as shown in Fig. S1e).

Supplementary deformation analyses and visual demonstrations (refer Fig. S1e and Video S1) confirm that the disc's conformity arises predominantly from its topology, with curvature adaptation governed by geometry-driven kinematics rather than only homogeneous material stretching. The synchronized rotation of ligaments, localized perimeter expansion, and smooth transition from a planar disc to a hemispherical profile collectively validate the auxetic-inspired and metamaterial-like deformation pathways. Thus, the rotational-unit ligament architecture, hinge-enabled expansion, and curvature-adaptive geometry accordingly reflect, the terms metamaterial-inspired and auxetic-inspired due to the geometric design philosophy and deformation mechanism highlighting this curvature-conformable ocular disc.

S2. Fabrication of Ocular Discs and Contact Lenses via 3D Printing

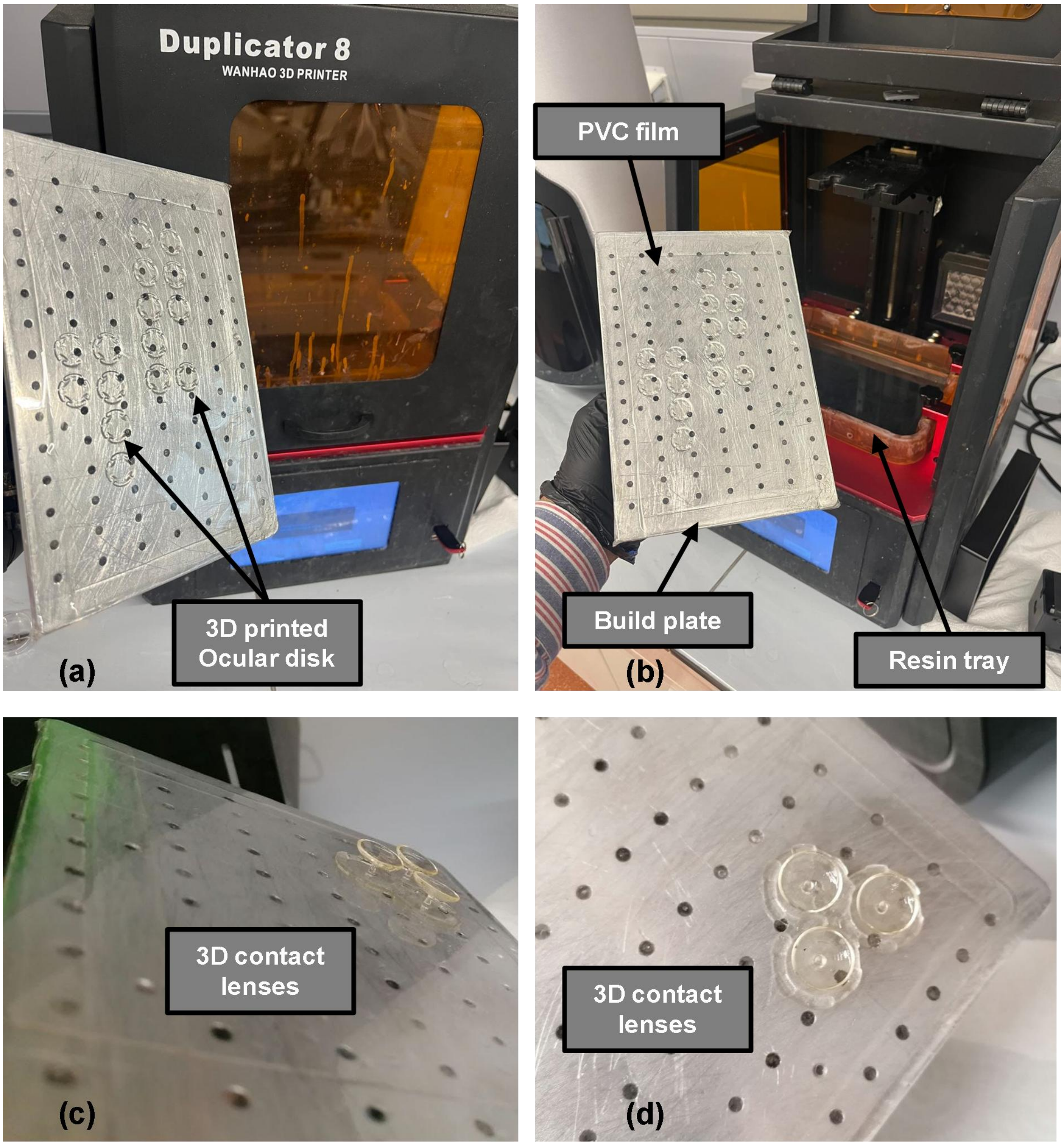

Figure S2: Close - up view of the (a-b) 3D printed ocular disc and (c-d) 3D-printed contact lenses on the build plate alongside the 3D printer used.

Table S1: Digital Light Processing (DLP) 3D Printing Parameters for Ocular Disc and Contact Lens Fabrication

Parameter	**Value / Setting**	**Unit**
Printer Model	Wanhao Duplicator D8	-
Light Wavelength	405	nm
Exposure Time (Burn-in Layers)	120	seconds
Exposure Time (Subsequent Layers)	80	seconds
Layer Thickness	35	µm
Build Plate Temperature	Ambient (25 ± 2)	°C
Post - Curing Time	10	minutes
Build Orientation	Horizontal	-

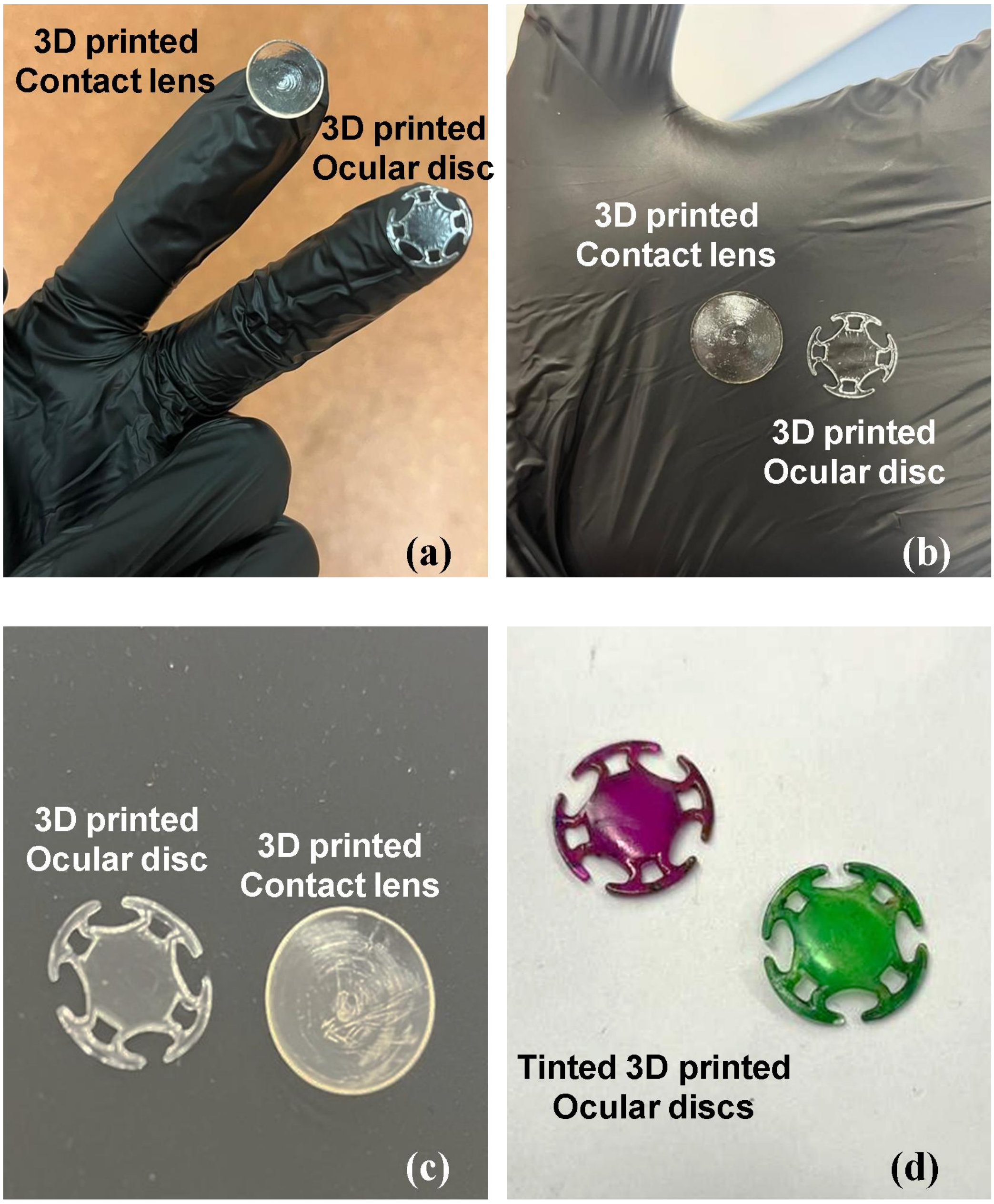

Figure S3: Representative visuals of the 3D-printed ocular disc and contact lenses: (a) Posterior surface suspended on a fingertip for scale, (b) flipped to display the anterior surface, (c) contrast enhanced image highlighting surface features, and (d) tinted ocular discs for improved visibility.

S3: Surface Roughness Characterization via Area Surface Scans: Comparison of Traditional Hemispherical and Flat Ocular 3D-Printed Lenses

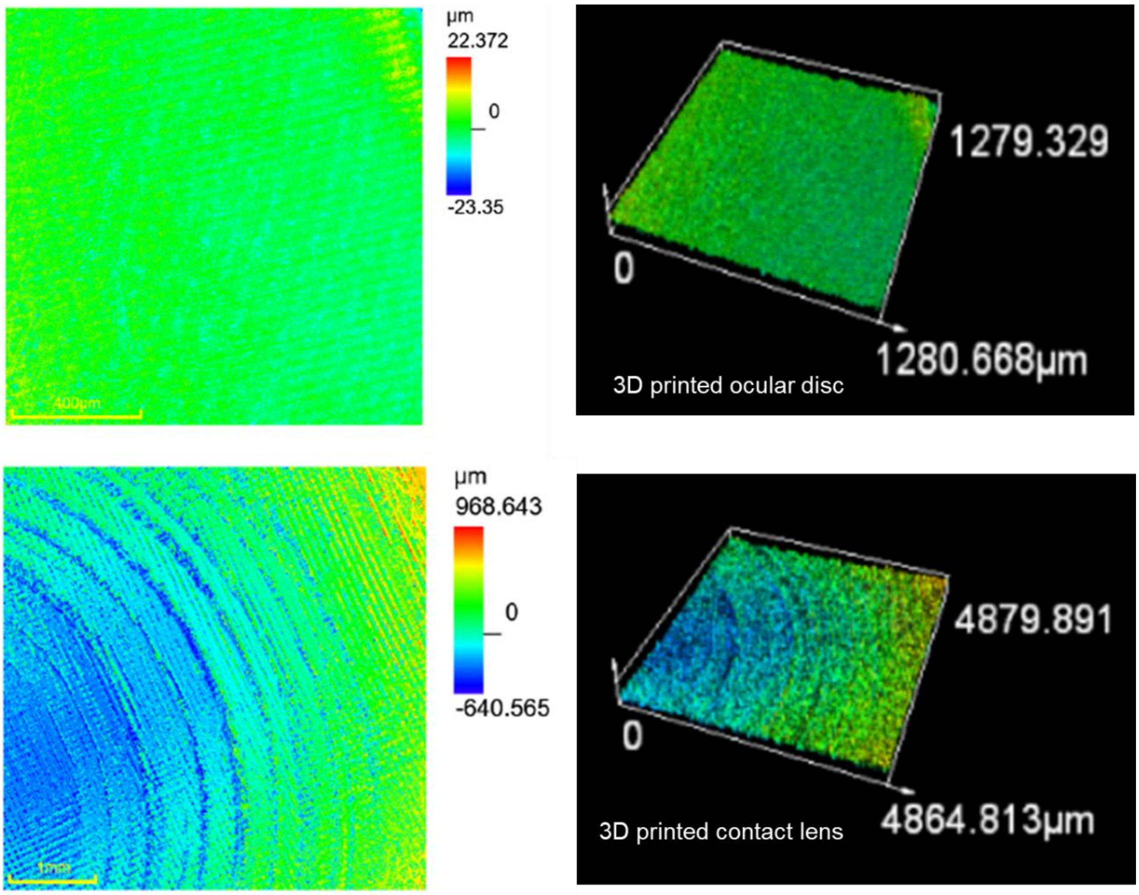

Figure S4: Laser profilometry-based surface area scans comparing the surface roughness of conventional 3D-printed hemispherical contact lenses with the proposed conformal auxetic-inspired metamaterial ocular discs.

Quantitative area-scan surface roughness analysis (refer Fig. S4) shows that the conformal auxetic-inspired metamaterial ocular disc exhibits a root mean square roughness (Sq) of 2.504 µm, compared to 185.92 µm for the 3D-printed hemispherical (curved) lens. This reduction of nearly 98 % demonstrates the effectiveness of the flat-printed ocular disc design in achieving markedly smoother surfaces and moving closer toward optical-grade quality.

S4. Setup for Contact angle measurement of Ocular Discs

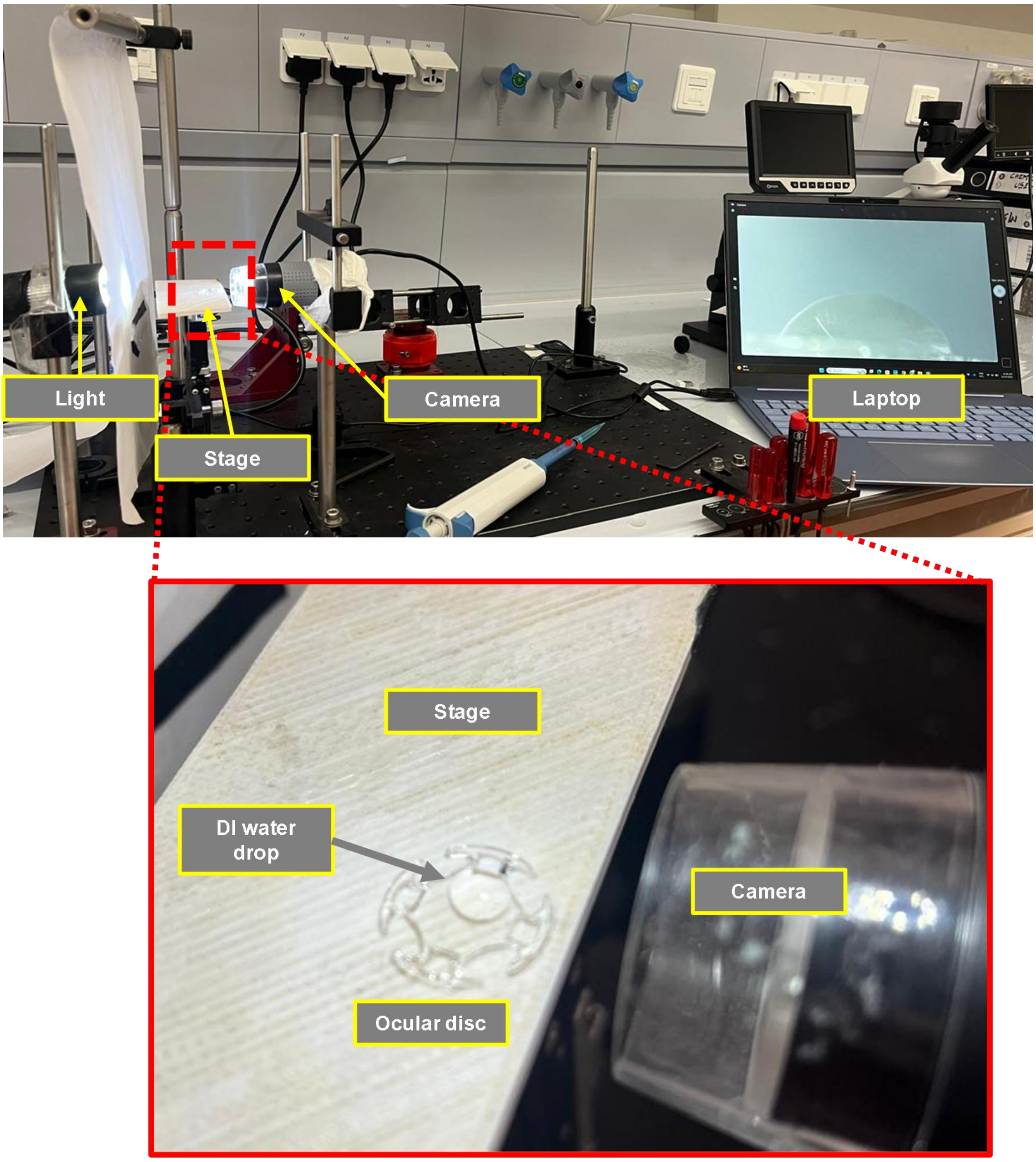

Figure S5: Experimental setup for contact angle measurement, including a close-up view of the water droplet on the ocular disc.

Table S2: Contact angle measurements

Trail	Hydrated	As printed
#1	64	67
#2	64.78	68
#3	65.1	66.3
Average	**64.63**	**67.1**
Error (±)	**0.5658**	**0.8544**

S5. Evaluation of Lens Fit and Resistance to Lifting Under Simulated Tear Pressure

This study introduces a new structural concept for a contact lens, an auxetic-inspired, metamaterial-based ocular disc that can be additively manufactured in a flat form yet conforms seamlessly to the hemispherical curvature of the eye as discussed in previous sections. While the design shows promising mechanical and functional behavior, future work must include extended biocompatibility assessments, and clinical-grade trials to further validate and refine its performance.

As a preliminary demonstration, we conducted simple interaction tests using phosphate-buffered saline (PBS), an artificial tear analogue, and recorded the results (Videos S4 – S6). First, the printed ocular disc was placed inside a Barron Artificial Anterior Chamber, a device typically used for corneal graft preparation. Using Syringe pump, PBS solution (5 mL, delivered at 100 mL/h) was introduced to simulate controlled tear loading. The disc remained securely positioned within the chamber while the PBS flowed uniformly across and out of the system, indicating that the lens can withstand tear-like dosing pressures and allow fluid permeability important for tear exchange, oxygen transport, and comfort during wear (Video S4).

Additional surface-loading tests showed that when PBS was applied directly from above, the disc again retained its structural integrity and position (Video S5). Finally, the lens was conformed onto a spherical eye model, pre-moistened with PBS. Upon loading the hydrated disc onto the model and dispensing PBS droplets using a variable-volume pipette, the lens maintained conformal contact yet was free to rotate and translate an essential functional requirement for natural ocular motion (reader is referred to Video S6).

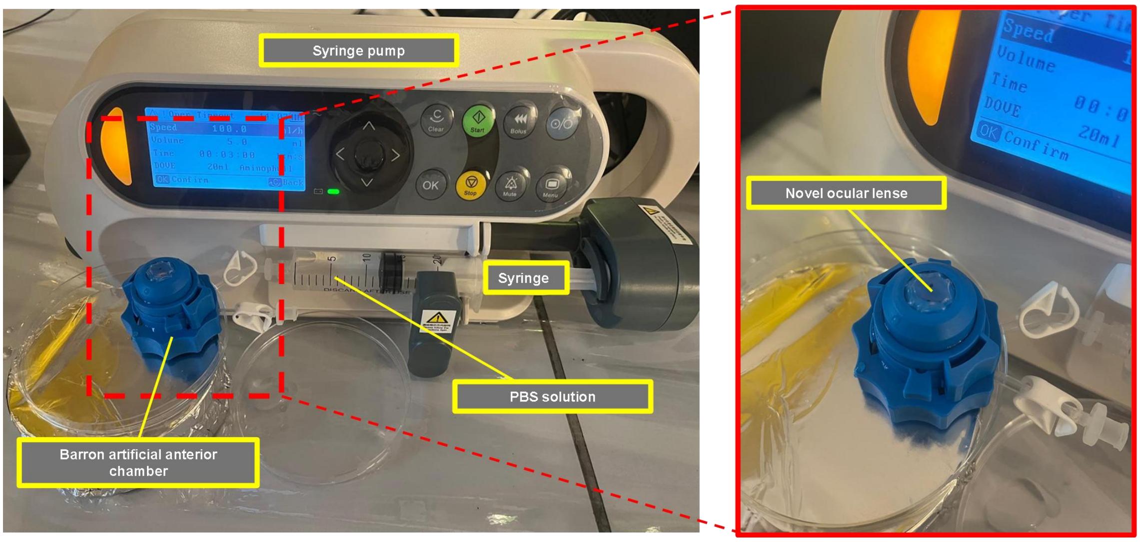

Figure S6: Experimental setup illustrating the characterization of the ocular lens response to controlled PBS solution loading and pressure interaction.

These demonstrations provide early evidence of the disc's conformability, stability under fluid interaction, and movement compatibility. More advanced characterizations, supported by clinical-grade facilities, will be pursued in future studies to comprehensively evaluate its suitability for ophthalmic applications.

S6. Setup for Optical Spectral analysis of Ocular Discs

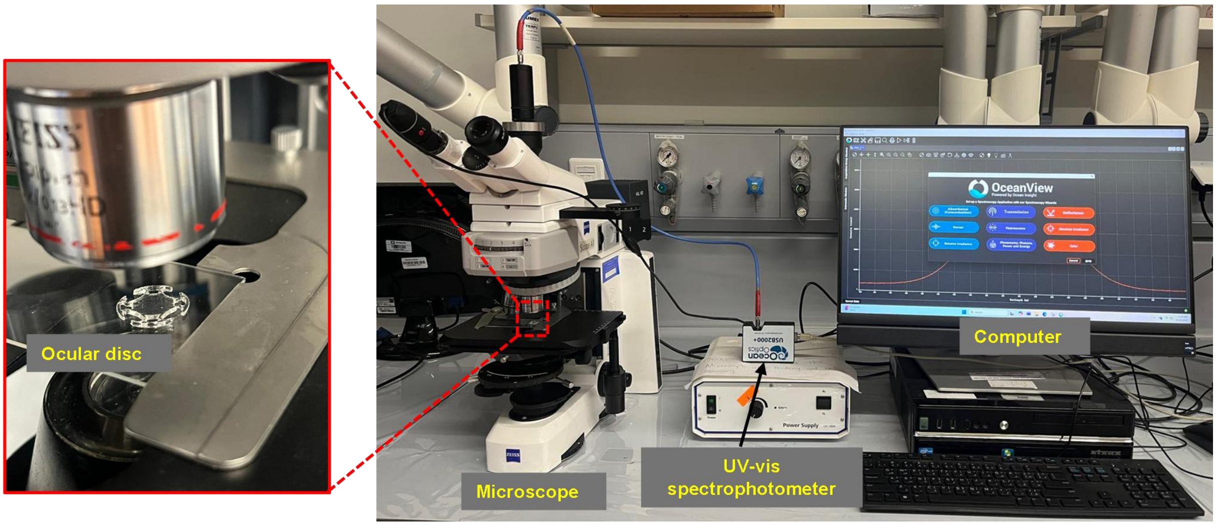

Figure S7: Experimental setup for spectral characterization of ocular discs, including a close-up view of the disc positioned for analysis

S7. Numerical Comparison of the proposed conformal metamaterial ocular disc with curved contact lens geometry

A simple linear elastic simulation was performed in ABAQUS to compare the existing contact lens with the proposed conformal auxetic-inspired metamaterial ocular disc design. Both models used a 0.15 mm tetrahedral mesh (see Fig. S8), with a Young’s modulus of 0.71 MPa. A mean pressure of 0.001 MPa (~8 mmHg) [4], was applied to mimic eyelid closure, while the inner surface was fixed. To reflect the eye blink's dynamic nature, a dynamic explicit step of 0.8 s is used. To accurately simulate the lens's behavior on the eye, the flat disc geometry was first computationally conformed to a standard corneal curvature before the eyelid pressure was applied. This preliminary study provides a basic comparison and may not fully replicate actual physiological conditions inside the eye.

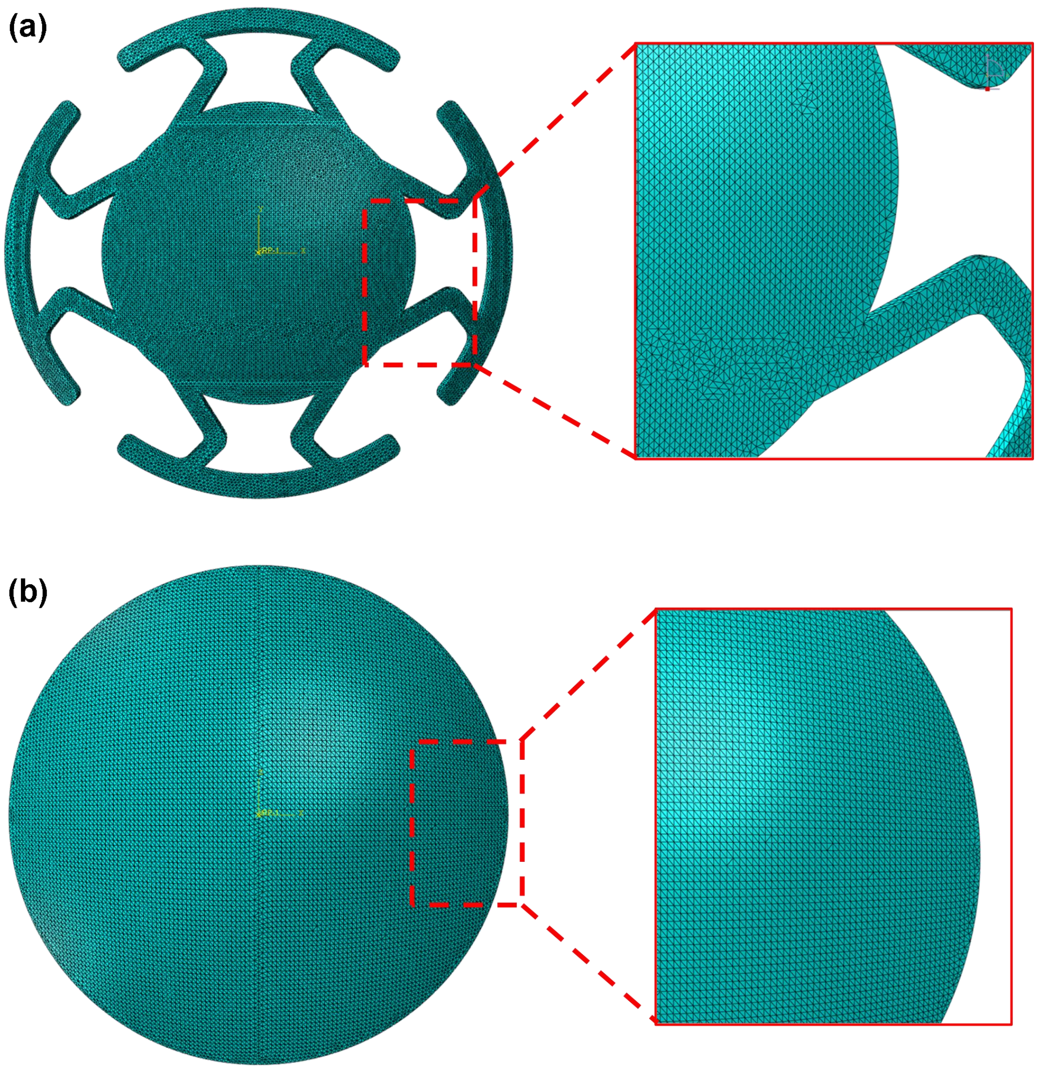

Figure S8: Finite element mesh representation of the (a) ocular disc and (b) contact lens models used in the simulation.

A conceptual finite element analysis was performed in ABAQUS to compare the stress distribution in the proposed conformal metamaterial ocular disc (top) with a conventional curved contact lens (bottom) under a uniform surface pressure of 0.001 MPa (see Fig. S9). The goal of this simulation was not to precisely predict in-vivo performance but to illustrate the effectiveness of the design in managing mechanical loads. The auxetic ocular disc exhibits a more uniform distribution of maximum principal stress, von Mises stress, and displacement magnitude, comparable to that of the conventional lens design. Notably, the uniform stress distribution within the circumferential ligament regions and the central vision-critical zone confirms the design's effectiveness in achieving its intended mechanical and functional goals. This outcome aligns with the design intent to safeguard the central optical zone while incorporating open-cell regions to enhance hydration and oxygen permeability upon corneal contact. In contrast, the conventional lens displays a more varied stress contour, particularly along its edges. The ocular disc's segmented and reinforced architecture facilitates efficient load redistribution, suggesting enhanced structural integrity, user comfort, and long-term durability. However, further validation under actual physiological conditions is essential to fully assess and optimize its performance.

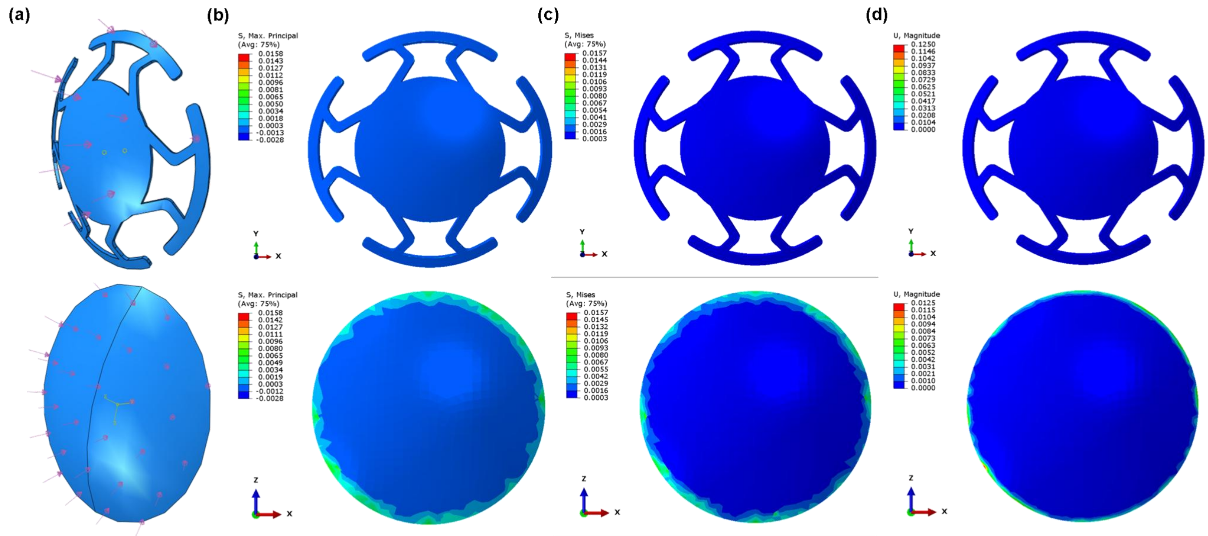

Figure S9: (a) Surface pressure applied as boundary condition; (b) Maximum principal stress; (c) Von Mises stress; and (d) Displacement magnitude distributions for the proposed auxetic ocular disc (top) and normal curved contact lens (bottom), as simulated in ABAQUS.

S8. Water content and swelling kinetics measurements

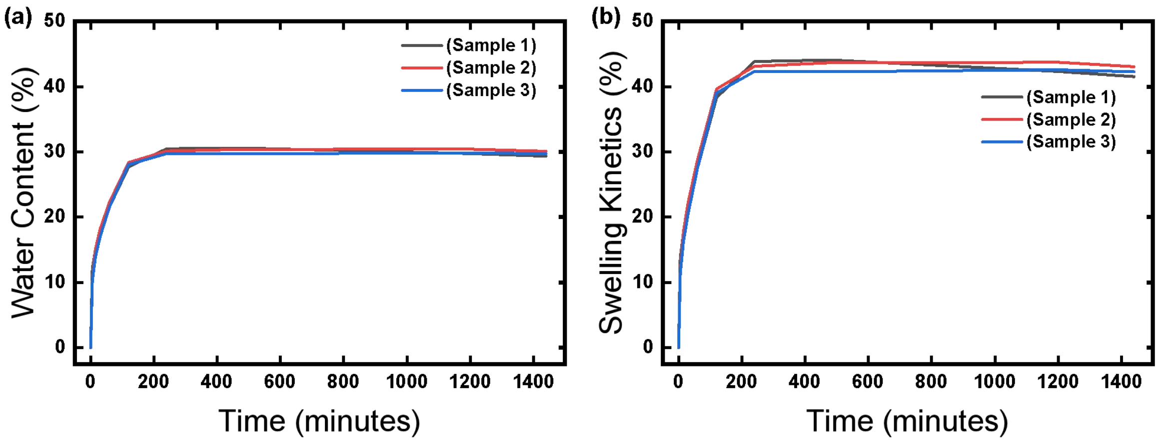

Figure S10: Repeatability assessment of (a) water content and (b) swelling kinetics measurements.

S9. Rheological Behavior

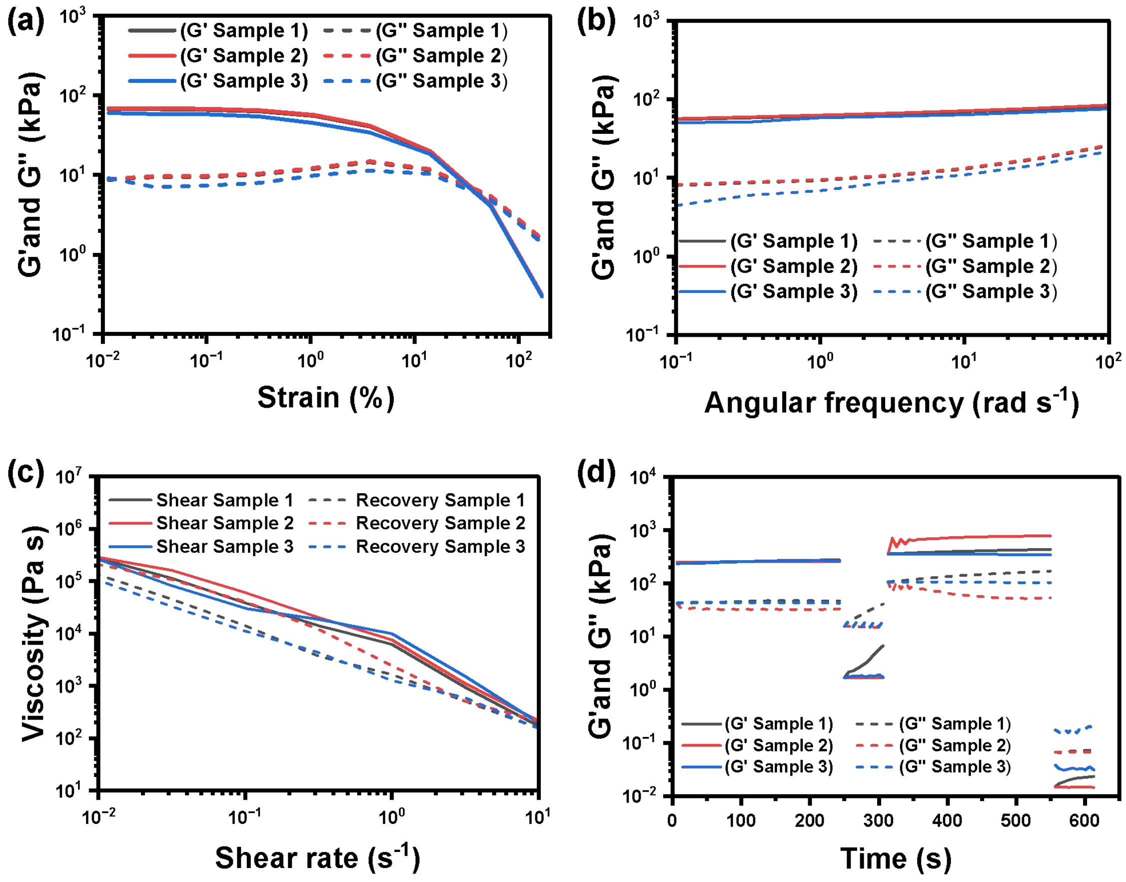

Figure S11: Repeatability analysis of rheological behavior: (a) strain-dependent oscillatory shear response, (b) frequency-dependent oscillatory shear behavior, (c) assessment of self-healing capability through step-strain tests alternating between 1 % and 500 % strain, and (d) demonstration of shear-thinning behavior and structural recovery under varying shear rates. (e) Experimental setup and the printed samples used for the rheological analysis.

S10. Mechanical Characterization

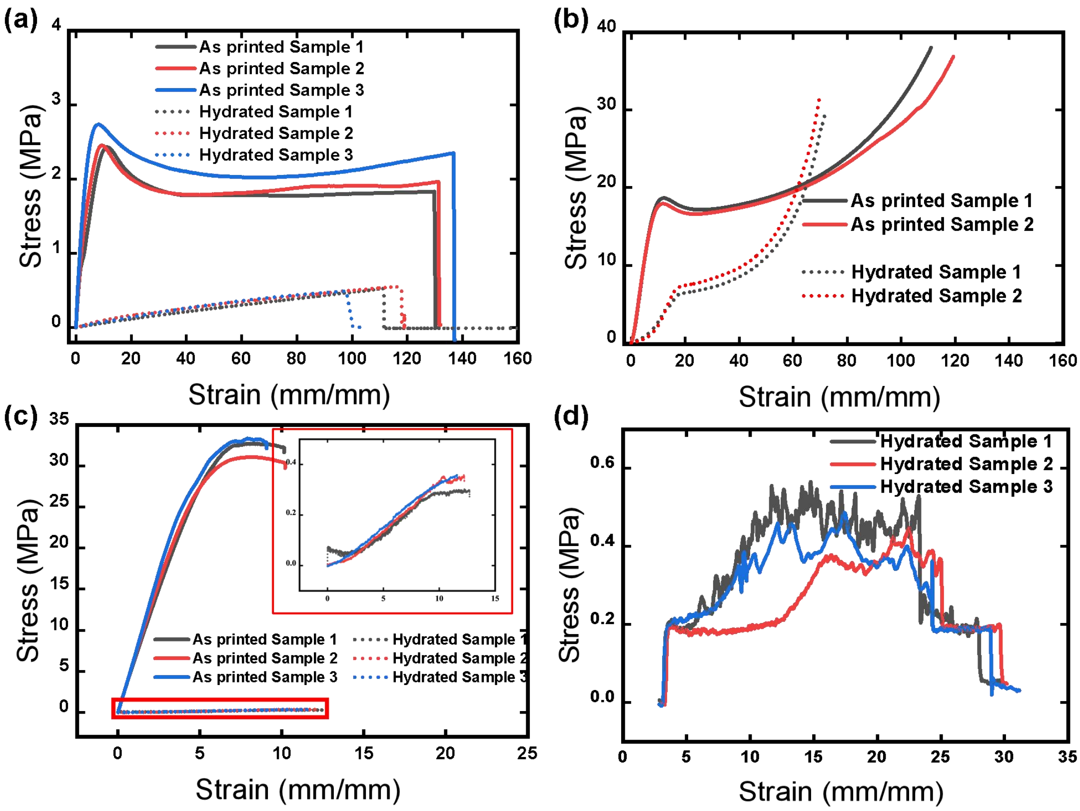

Figure S12: Repeatability analysis of mechanical tests conducted under (a) tensile loading, (b) compressive loading, (c) three-point bending (flexural), and (d) tear resistance.

References

[1] M. P. Do Carmo, Differential geometry of curves and surfaces: revised and updated second edition. Courier Dover Publications, 2016.

[2] A. H. Robinson, J. L. Morrison, P. C. Muehrcke, A. J. Kimerling, and S. C. Guptill, “Elements of Cartography--6th Ed, 544 pp,” New York, John Willey & Sons, 1995.

[3] J. P. Snyder, Map projections--A working manual, vol. 1395. US Government Printing Office, 1987.

[4] A. J. Shaw, M. J. Collins, B. A. Davis, and L. G. Carney, “Eyelid pressure and contact with the ocular surface,” Investig. Ophthalmol. & Vis. Sci., vol. 51, no. 4, pp. 1911–1917, 2010.